Comparison of Cascaded Backstepping Control Approaches with Hysteresis Compensation for a Linear Axis with Pneumatic Muscles

Dominik Schindele * **Harald Aschemann** *

* *Chair of Mechatronics, University of Rostock, Germany, (email: {dominik.schindele,harald.aschemann}@uni-rostock.de)*

Abstract: This paper presents two control approaches for a linear axis with pneumatic muscles. Its guided carriage is driven by a nonlinear drive system consisting of two pulley tackles with pneumatic muscle actuators arranged at both sides. This innovative drive concept allows for an increased workspace as well as higher carriage velocities as compared to a direct actuation. Both proposed control schemes have a cascaded structure, where the control design is based on backstepping techniques. Hysteresis in the force characteristic of the pneumatic muscles is considered by an asymmetric shifted Prandtl-Ishlinskii model, while remaining uncertainties are compensated using an adaptive backstepping strategy. The main difference between both approaches is the usage of either the internal muscle pressures or the muscle forces as controlled variables of the inner control loops. Both control approaches have been implemented on a test-rig and show an excellent closed-loop performance.

Keywords: pneumatic muscles, backstepping control, hysteresis modelling, disturbance compensation, mechatronics.

1. INTRODUCTION

Pneumatic muscles are innovative tensile actuators consisting of a fibre-reinforced vulcanised rubber tubing with appropriate connectors at both ends. The working principle is based on a rhombical fibre structure that leads to a muscle contraction in longitudinal direction when the pneumatic muscle is filled with compressed air. This contraction can be used for actuation purposes. Pneumatic muscles are low cost actuators and offer several further advantages in comparison to classical pneumatic cylinders: significantly less weight, no stick-slip effects, insensitivity to dirty working environment, and a higher force-to-weight ratio. A major advantage of pneumatic drives as compared to electrical drives is their capability of providing large maximum forces for a longer period of time. In this case electrical drives are at risk of overheating and may result in increased errors due to thermal expansion. For these reasons, different researchers have investigated pneumatic muscles as actuators for several applications, e.g. a planar elbow manipulator in Lilly and Yang [2005], a two degree-of-freedom serial manipulator in Van-Damme et al. [2007] or a parallel manipulator in Zhu et al. [2008].

However, pneumatic muscles are also subject to some drawbacks: They show a slower time response at force-generating compared to electrical drives, and they are characterised by dominant nonlinearities, namely the force characteristic and the volume characteristic. As a consequence, these nonlinearities have to be considered at control design. In this contribution pneumatic muscles are employed to actuate a novel linear drive, at which the muscle force is transmitted to the carriage by a pulley tackle consisting of a wire rope and several deflection pulleys, see Fig. 1. This pneumatic linear drive allows for maximum velocities of approximately 1.3 m/s in a workspace of approximately 1 m. Hence, the velocities and the workspace are enlarged by a factor of three in comparison to a linear

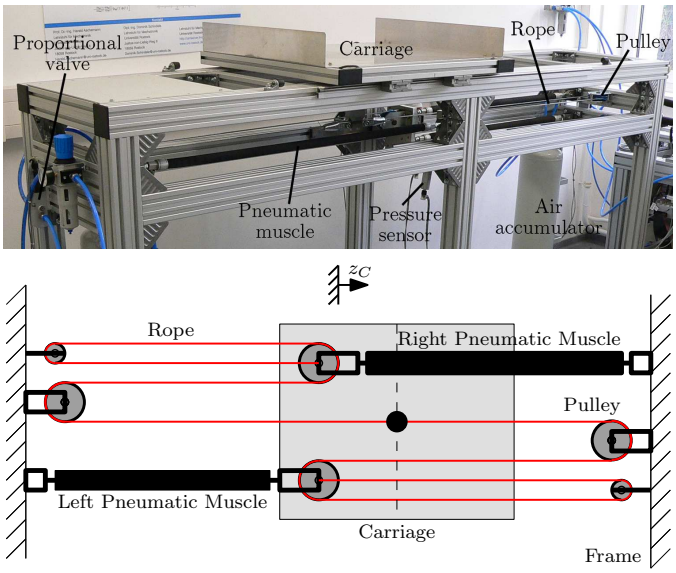

Fig. 1. Experimental setup.

axis directly actuated by the pneumatic muscles as presented in Krichel et al. [2010]. For the actuation of the carriage, four pneumatic muscles are employed, whereas two muscles are used for each tension direction, respectively. For control of the test rig a cascaded backstepping control is proposed. In earlier work,cf. Aschemann and Schindele [2008], as well as in the major part of published control applications using pneumatic muscles, the internal pressures of the muscles are used as control inputs of the outer loop and are controlled in a fast underlying control loop. Alternatively, there is the possibility of controlling the muscle forces in an underlying control loop. For this reason two control approaches for the linear axis with pneumatic muscles are compared in this contribution. In one

of these the muscle pressures are controlled in an underlying control loop, as in earlier work, whereas in the other approach the muscle forces represent the variables to be controlled in the underlying loop. In the outer control loop the carriage position and the mean muscle pressure or the mean muscle force represent the controlled variables.

The paper is structured as follows: First, a control-oriented model of the pneumatically driven high-speed linear axis is derived in sections 2, 3 and 4 as a basis for the control design. For this purpose, polynomial descriptions are utilised to describe the nonlinear characteristics of the pneumatic muscle, i.e., the muscle volume and the muscle force as functions of both contraction length and internal muscle pressure. The hysteresis in the force characteristics of the muscles is modelled by a modified Prandtl-Ishlinskii model. Second, two cascaded control structures are designed for the linear axis, in section 5. The outer control loop achieves a precise tracking of the carriage position and the mean muscle pressure or the mean muscle force. The inner loop involves either a fast control of the muscle pressures or a fast control of the muscle forces. Remaining model uncertainties are estimated and compensated by an adaptive control action. Finally, in section 6, the proposed control strategies have been implemented and investigated at the test-rig of the Chair of Mechatronics, University of Rostock. Thereby, desired trajectories for the carriage position can be tracked with high accuracy.

2. MODELLING OF THE MECHANICAL SUBSYSTEM

The modelling of the pneumatically driven high-speed linear axis involves the mechanical subsystem and the pneumatic subsystem, which are coupled by the tension forces of the pneumatic muscles. The control-oriented mechanical model of the high-speed linear axis consists of the carriage and two pulley tackles, at which one pulley tackle transmits the tension force of two pneumatic muscles to the carriage in each case. As for modelling, the mechanical subsystem is divided into the following elements: a lumped mass for the carriage (mass m_C), the two connection plates, which are also modelled as lumped masses (mass $m_{MFi},\ i=\{l,r\}$) and the six pulleys (mass moment of inertia $J_{ij},\ i=\{l,r\},\ j=\{1,2,3\}$). As the rope deflection is negligible, the motion of the linear axis is completely described by the generalised coordinate $z_C(t)$, which denotes the carriage position. The equation of motion directly follows from Newton's second law in the form of a nonlinear second-order differential equation

$$m\ddot{z}_C = \frac{a_M}{k}\left[F_{Mr}\left(p_{Mr},\Delta\ell_{Mr}\right) - F_{Ml}\left(p_{Ml},\Delta\ell_{Ml}\right)\right] - F_U\ , \quad (1)$$

with the reduced mass

$$m = m_C + \frac{m_{MFl}}{k^2} + \frac{m_{MFr}}{k^2} + \sum_{j=1}^{3}\left[\frac{J_{lj}}{k^2}\left(\frac{j}{r}\right)^2 + \frac{J_{rj}}{k^2}\left(\frac{j}{r}\right)^2\right]\ . \quad (2)$$

The parameter $k=3$ denotes the number of pulleys employed for each pulley tackle. The parameter $a_M=2$ stands for the two muscles used for the actuation in the left or right direction, respectively, and which are characterised by a nonlinear force characteristic $F_{Mi},\ i=\{l,r\}$ depending on the internal muscle pressure p_{Mi} and the contraction length $\Delta\ell_{Mi}$. All remaining model uncertainties are taken into account by the resulting disturbance force F_U.

3. MODELLING OF THE MUSCLE FORCE

The force characteristic F_{Mi} of a pneumatic muscle states the resulting tension force for given internal pressure p_{Mi} as well as given contraction length $\Delta\ell_{Mi}$ and represents the connection of the mechanical and the pneumatic system part. As the force characteristic of a pneumatic muscle shows a hysteresis depending on the contraction length $\Delta\ell_{Mi}$, see Schindele and Aschemann [2012] or Vo-Minh et al. [2011], for modelling, the nonlinear muscle force is divided in two parts: the static muscle force $F_{Mi,st}$ as well as the hysteresis part $F_{Mi,hys}$. Then, the complete force characteristic F_{Mi} can be stated as

$$F_{Mi} = F_{Mi,st} + F_{Mi,hys}\ . \quad (3)$$

The static force characteristic has been identified by measurements, see Schindele [2013], and, then, approximated by the following polynomial description

$$F_{Mi,st}(p_{Mi},\Delta\ell_{Mi}) = \begin{cases} \bar{F}_{Mi}(p_{Mi},\Delta\ell_{Mi}) & \text{if } \bar{F}_{Mi}>0 \\ 0 & \text{else} \end{cases}\ , \quad (4a)$$

$$\bar{F}_{Mi}(p_{Mi},\Delta\ell_{Mi}) = \underbrace{\sum_{m=0}^{3}\left(a_m\Delta\ell_{Mi}^m\right)}_{=f_{1i}(\Delta\ell_{Mi})}p_{Mi} - \underbrace{\sum_{n=0}^{4}\left(b_n\Delta\ell_{Mi}^n\right)}_{=f_{2i}(\Delta\ell_{Mi})}\ . \quad (4b)$$

Given the initial contraction length ℓ_{M0} of the pneumatic muscles, the contraction length of the left and right pneumatic muscle are determined by the following relations

$$\Delta\ell_{Ml} = \ell_{M0} - \frac{1}{k}z_C\ ,\quad \Delta\ell_{Mr} = \ell_{M0} + \frac{1}{k}z_C\ . \quad (5)$$

The muscle hysteresis is modelled by an asymmetric shifted Prandtl-Ishlinskii (ASPI) model as proposed in Li et al. [2012]. The Prandtl-Ishlinskii model is a widely used mathematical model for description of hysteresis and represents a subset of Preisach models, cf. Mayergoyz [1986]. Whereas the classical Prandtl-Ishlinskii model is not able to describe asymmetric hysteresis curves, the ASPI model addresses this problem. The Prandtl-Ishlinskii model is stated in the discrete-time domain and describes hysteresis using a superposition of elementary play-operators, see Kuhnen [2003]. With the sampling time T, the output $y_j(k)$ of one play-operator at the time $t_k=kT$ is a function of the carriage position as input $z_C(k)$

$$y_j(k) = \max\{z_C(k)-r_j, \min\{z_C(k)+r_j, y_j(k-1)\}\}\ , \quad (6)$$

with the initial condition

$$y_j(0) = \max\{z_C(0)-r_j, \min\{z_C(0)+r_j, y_{j0}\}\}\ . \quad (7)$$

Here, the initial state y_{j0} and the threshold r_j are introduced as parameters for characterisation of the corresponding play-operator $j,\ j=\{1,..,N\}$. For the ASPI model an additional shift operator, similar to the play-operator is introduced

$$\Psi_l(k) = \max\{c_l z_C(k), \min\{z_C(k), y_l(k-1)\}\}\ , \quad (8)$$

$$\Psi_l(0) = \max\{c_l z_C(0), \min\{z_C(0), y_{l0}\}\}\ , \quad (9)$$

with the positive constant $c_l>0$. For a finite number N of play-operators and a finite number M of shift operators the ASPI model calculates the hysteresis force as the weighted summation of the individual operators

$$F_{M,hys}(k) = \sum_{j=1}^{N} w_j y_j(k) + \sum_{l=1}^{M} v_l \Psi_l + g(z_C(k))\ . \quad (10)$$

Here, $g(z_C(k))$ is a Lipschitz continuous function. Although the accuracy of the hysteresis model can be improved with an increasing number of play operators and shift operators,

the number of parameters that have to be identified becomes larger as well. Hence, a system-specific trade-off between the model accuracy and the number of parameters to be identified is necessary. Here, $N = 4$ play operators and $M = 3$ shift operators have been chosen.

4. DYNAMICS OF THE PNEUMATIC ACTUATORS

The dynamics of the internal muscle pressure follows directly from a mass balance for the compressed air in the muscle. As the internal muscle pressure is limited by a maximum value of $p_{Mi,max} = 7$ bar, the ideal gas equation represents an accurate description of the thermodynamic behaviour of the air in the left or right muscle, respectively. The thermodynamic process is modelled as a polytropic change of state with $n = 1.26$ as identified polytropic exponent. The resulting state equation for the internal muscle pressure in the muscle i is given by (cf. Schindele [2013] for further details)

$$\begin{aligned}\dot{p}_{Mi} &= \frac{n}{V_{Mi} + n\frac{\partial V_{Mi}}{\partial p_{Mi}} p_{Mi}} \left[R_L\, T_{Mi}\, \dot{m}_{Mi} - \frac{\partial V_{Mi}}{\partial \Delta\ell_{Mi}} \frac{\mathrm{d}\Delta\ell_{Mi}}{\mathrm{d}z_C} \dot{z}_C\, p_{Mi} \right] \\ &= k_{ui}\left(\Delta\ell_{Mi}, p_{Mi}\right) \dot{m}_{Mi} - k_{pi}\left(\Delta\ell_{Mi}, \Delta\dot{\ell}_{Mi}, p_{Mi}\right) p_{Mi} \,, \end{aligned} \tag{11}$$

where R_L represents the gas constant of air. The internal temperature T_{Mi} can be approximated with good accuracy by the constant temperature of the ambiance. The volume characteristic of the pneumatic muscle can be accurately approximated by the polynomial function

$$V_{Mi}\left(\Delta\ell_{Mi}, p_{Mi}\right) = \sum_{k=0}^{3} \left(a_k \Delta\ell_{Mi}^k \right) p_{Mi} + \sum_{l=0}^{3} b_l \Delta\ell_{Mi}^l \,, \tag{12}$$

where the coefficients a_k and b_l have been identified by measurements, cf. Schindele [2013].

5. CASCADED CONTROL DESIGN

For control design of the high-speed linear axis, a cascaded control structure has been chosen. Either the internal muscle pressures $p_{Mi},\ i = \{l,r\}$, or the muscle forces $F_{Mi},\ i = \{l,r\}$ are controlled in a fast underlying control loop, whereas the carriage position z_C as well as the mean muscle pressure $p_M = 0.5\,(p_{Ml} + p_{Mr})$ or the mean muscle force $F_M = 0.5\,(F_{Ml} + F_{Mr})$ represent the controlled variables of the outer loop. The control design for both the outer control loop and the inner control loop are realised by backstepping techniques, cf. Krstić et al. [1995]. The detailed design procedure is explained in Schindele [2013]. The backstepping approach also allows for an estimation of unknown parameters after an extension, and it is called adaptive backstepping then. Here, the adaptive backstepping approach is used to estimate the remaining disturbance force F_U. For control design, the differential flatness property of the system under consideration has been exploited, cf. Fliess et al. [1995] or Aschemann and Schindele [2008]. In this manner, the nonlinearities of the controlled system can be compensated by the inverse dynamics and only the trajectory error system has to be stabilised by backstepping techniques.

5.1 Control implementation with underlying pressure control

For control implementation with underlying pressure control the flat outputs of the outer control loop are the carriage position $y_1 = z_C$ and the mean muscle pressure $y_2 = p_M$. Subsequent differentiations of the first flat output until the input variables appear lead to

$$\begin{aligned} y_1 &= z_C \,,\ \dot{y}_1 = \dot{z}_C \,, \\ \ddot{y}_1 &= \frac{a_M}{k\,m} \left[f_{1r}\, p_{Mr} - f_{2r} + F_{Mr,hys} \right. \\ &\qquad \left. - f_{1l}\, p_{Ml} + f_{2l} - F_{Ml,hys} \right] - \frac{F_U}{m} \end{aligned} \tag{13}$$

whereas the second flat output depends directly on the internal muscle pressures as input variables

$$y_2 = p_M = \frac{1}{2}\left(p_{Ml} + p_{Mr}\right) \,. \tag{14}$$

By solving (13) and (14) for the internal muscle pressures, the inverse dynamics results in

$$\begin{aligned} u = \begin{bmatrix} p_{Ml} \\ p_{Mr} \end{bmatrix} &= \frac{1}{f_{1l} + f_{1r}} \\ &\cdot \begin{bmatrix} f_{2l} - f_{2r} - \frac{k\,m}{a_M}\upsilon_1 + 2\,p_M\,f_{1r} - F_{Ml,hys} + F_{Mr,hys} \\ f_{2r} - f_{2l} + \frac{k\,m}{a_M}\upsilon_1 + 2\,p_M\,f_{1l} + F_{Ml,hys} - F_{Mr,hys} \end{bmatrix} . \end{aligned} \tag{15}$$

As control input $\upsilon_1 = \ddot{z}_C + \frac{F_U}{m}$ the carriage acceleration corrected by the disturbance term $\frac{F_U}{m}$ is chosen. Then, the backstepping control law as well as the differential equation for the disturbance estimation result in

$$\upsilon_1 = \ddot{z}_{Cd} + g_1\left(e_1, e_2\right) + c_3\, e_2 + c_4\, e_2^3 + \frac{\hat{F}_U}{m} \,, \tag{16}$$

$$\dot{\hat{F}}_U = \frac{e_2\,\gamma}{m} \,, \tag{17}$$

with

$$\begin{aligned} e_1 &= z_{Cd} - z_C \,, \\ e_2 &= c_1\, e_1 + c_2\, e_1^3 + \dot{e}_1 \,, \\ g_1 &= e_1\left(1 - c_1^2\right) + e_2\left(c_1 + 3\,c_2\, e_1^2\right) - 4\,c_1\,c_2\, e_1^3 - 3\,c_2^2\, e_1^5 \,. \end{aligned} \tag{18}$$

Here, c_1, c_2, c_3, c_4 and γ are positive control design parameters. By considering these equations, it can be shown that the time derivative of the control Lyapunov function

$$V_1(e_1, e_2) = \frac{1}{2}\, e_1^2 + \frac{1}{2}\, e_2^2 + \frac{1}{2\,\gamma}\left(F_U - \hat{F}_U\right)^2 \tag{19}$$

is negative semidefinite, see Schindele [2013]. However, the invariance principle of LaSalle, cf. LaSalle and Lefschetz [1961], can be employed to prove global asymptotic stability, cf. Krstić et al. [1995].

The input variables $p_{Mi},\ i = \{l,r\}$, of the outer loop serve as desired values of the controlled variables of the inner control loop, cf. Fig. 2. For the underlying control of the muscle pressures the first time derivatives of the desired muscle pressures are required additionally. Here, these variables are calculated from desired values exploiting the differential flatness of the system. For this purpose, the third time derivative of the first output variable $y_1 = z_C$ and the first time derivative of the second output variable $y_2 = p_M$ are considered

$$\begin{aligned} \dddot{y}_1 &= \frac{a_M}{k\,m} \left[\dot{F}_{Mr}\left(p_{Mr}, \dot{p}_{Mr}, \Delta\ell_{Mr}, \Delta\dot{\ell}_{Mr}\right) \right. \\ &\qquad \left. - \dot{F}_{Ml}\left(p_{Ml}, \dot{p}_{Ml}, \Delta\ell_{Ml}, \Delta\dot{\ell}_{Ml}\right) \right] - \frac{1}{m}\dot{F}_U \,, \end{aligned} \tag{20}$$

$$\dot{y}_2 = \frac{1}{2}\left(\dot{p}_{Ml} + \dot{p}_{Mr}\right) . \tag{21}$$

Solving (20) and (21) for the variables $\dot{p}_{Mi}$, the time derivatives of the desired muscle pressures can be stated as functions of desired values

$$\begin{bmatrix} \dot{p}_{Mld} \\ \dot{p}_{Mrd} \end{bmatrix} = \begin{bmatrix} \dot{p}_{Mld}\left(z_{Cd}, \dot{z}_{Cd}, \dddot{z}_{Cd}, p_{Mld}, p_{Mrd}, \dot{p}_{Md}, \dot{F}_U\right) \\ \dot{p}_{Mrd}\left(z_{Cd}, \dot{z}_{Cd}, \dddot{z}_{Cd}, p_{Mld}, p_{Mrd}, \dot{p}_{Md}, \dot{F}_U\right) \end{bmatrix} . \tag{22}$$

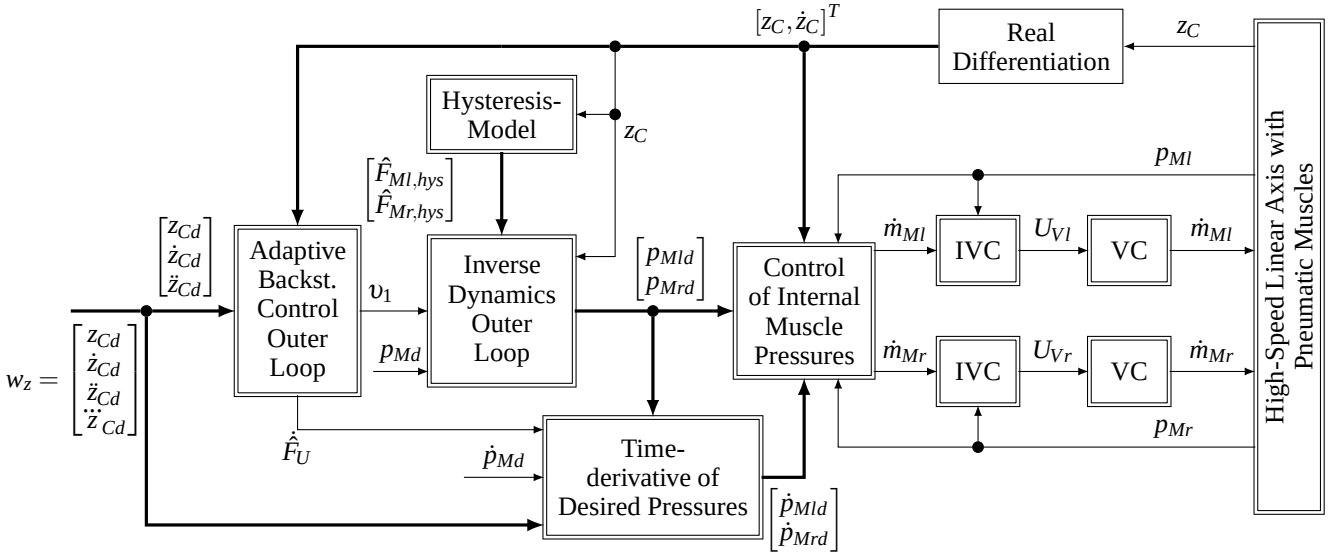

Fig. 2. Block diagram of the cascaded control structure: the muscle pressures are controlled in a fast underlying control loop, whereas the carriage position as well as the mean muscle pressure are controlled in an outer loop.

The control law of the underlying control loop, which represents a fast control of the corresponding internal muscle pressure p_{Mi}, is designed similarly to that of the outer control loop. Considering (11), the inverse dynamics for the pneumatic subsystem can be stated as

$$\dot{m}_{Mi} = \frac{1}{k_{ui}\left(\Delta\ell_{Mi}, p_{Mi}\right)}\left[\upsilon_{Mi} + k_{pi}\left(\Delta\ell_{Mi}, \Delta\dot{\ell}_{Mi}, p_{Mi}\right) p_{Mi}\right] , \quad (23)$$

with the internal muscle pressure p_{Mi} as flat output. The first time derivative of the flat output $\upsilon_{Mi} = \dot{p}_{Mi}$ can be chosen as stabilising control input. Then, the following stabilising control law for the pressure control

$$\upsilon_{Mi} = \dot{p}_{Mid} + a_i\left(p_{Mid} - p_{Mi}\right) , \quad (24)$$

where the positive control design parameter $a_i > 0$ guarantees a negative definite time derivative of the control Lyapunov function

$$V_2 = \frac{1}{2}\left(p_{Mid} - p_{Mi}\right)^2 . \quad (25)$$

The complete control structure is depicted in Fig. 2. Here, the nonlinear valve characteristics (VC) of the left and the right proportional valve is compensated by its approximated inverse characteristics (IVC), which provides the valve voltage U_{Vi}.

5.2 Control implementation with underlying force control

In contrast to the underlying pressure control, also the muscle forces can be controlled in a underlying loop. The control structure remains almost the same. In an outer control loop the carriage position and the mean muscle force are the controlled variables, whereas the muscle forces are controlled in fast underlying control loops and used as control inputs of the outer loop. In this case, the outer loop shows a linear behaviour. The carriage position $y_1 = z_C$ is chosen as the first of two flat outputs. Then, the second time derivative depends on the left and the right muscle force as input variables

$$\begin{aligned} &y_1 = z_C \ , \ \dot{y}_1 = \dot{z}_C \ , \\ &\ddot{y}_1 = \ddot{z}_C = \frac{a_M}{k\,m}\left[F_{Mr} - F_{Ml}\right] - \frac{F_U}{m} . \end{aligned} \quad (26)$$

The mean muscle force as second flat output directly depends on the input variables

$$y_2 = F_M = \frac{1}{2}\left(F_{Ml} + F_{Mr}\right) . \quad (27)$$

Considering (26) and (27) the inverse dynamics results in

$$u = \begin{bmatrix} F_{Ml} \\ F_{Mr} \end{bmatrix} = \frac{1}{2\,a_M}\begin{bmatrix} 2\,a_M F_M - k\,m\left(\ddot{z}_C + \frac{F_U}{m}\right) \\ 2\,a_M F_M + k\,m\left(\ddot{z}_C + \frac{F_U}{m}\right) \end{bmatrix} . \quad (28)$$

As the trajectory error system is the same as in the case of an underlying pressure control, the control law as well as the differential equation for estimating the disturbances are calculated by (16) and (17). The time derivatives of the desired input variables $\dot{F}_{Mid}$ can be computed as follows

$$\dddot{y}_1 = \dddot{z}_C = \frac{a_M}{k\,m}\left[\dot{F}_{Mr} - \dot{F}_{Ml}\right] - \frac{1}{m}\dot{F}_U , \quad (29)$$

$$\dot{y}_2 = \dot{F}_m = \frac{1}{2}\left(\dot{F}_{Ml} + \dot{F}_{Mr}\right) . \quad (30)$$

Solving (29) and (30) for $\dot{F}_{Ml}$ and $\dot{F}_{Mr}$ and evaluating the solution with desired variables leads to

$$\begin{bmatrix} \dot{F}_{Mld} \\ \dot{F}_{Mrd} \end{bmatrix} = \frac{1}{2\,a_M}\begin{bmatrix} 2\,a_M \dot{F}_{md} - k\,m\left(\dddot{z}_{Cd} + \frac{\dot{F}_U}{m}\right) \\ 2\,a_M \dot{F}_{md} + k\,m\left(\dddot{z}_{Cd} + \frac{\dot{F}_U}{m}\right) \end{bmatrix} . \quad (31)$$

For the underlying force control the muscle force $y_i = F_{Mi}$ is chosen as flat output. Considering (4) yields

$$\dot{y}_i = \dot{F}_{Mi} = f_{1i}\,\dot{p}_{Mi} + \dot{f}_{1i}\,p_{Mi} - \dot{f}_{2i} . \quad (32)$$

In combination with (11) the inverse dynamics can be stated as

$$\dot{m}_{Mi} = \frac{f_{1i}\,k_{pi}\,p_{Mi} - \dot{f}_{1i}\,p_{Mi} + \dot{f}_{2i} + \upsilon_i}{f_{1i}\,k_{ui}} . \quad (33)$$

Employing $\upsilon_i = \dot{F}_{Mi}$ as control input, the following control law can be used to stabilise the error dynamics asymptotically

$$\upsilon_i = \dot{F}_{Mid} + a_i\left(F_{Mid} - F_{Mi}\right) , \quad (34)$$

with $a_i > 0$. This control law leads to a negative definite time derivative of the control Ljapunov function

$$V_i = \tfrac{1}{2}\left(F_{Mid} - F_{Mi}\right)^2 . \quad (35)$$

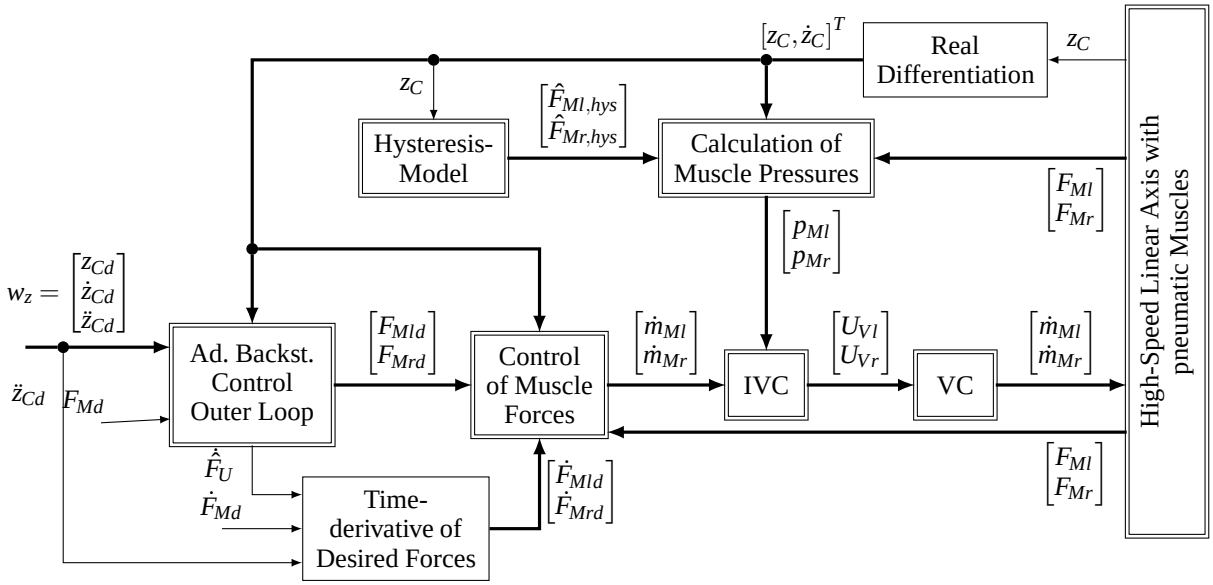

Fig. 3. Block diagram of the cascaded control structure: the muscle forces are controlled in a fast underlying control loop, whereas the carriage position as well as the mean muscle force are controlled in an outer loop.

The corresponding control structure is depicted in Fig. 3. The measured forces are the overall forces, already including the hysteresis. Hence, a additional hysteresis compensation action is not needed. However, the inverse valve characteristics depends on the internal muscle pressure, which is not measured in this case, but calculated from the muscle forces as follows

$$p_{Mi} = \frac{F_{Mi,ges} + f_{2i} - F_{Mi,hys}}{f_{1i}} \,. \tag{36}$$

Thus, hysteresis modelling makes sense also in the case of muscle force control.

6. EXPERIMENTAL RESULTS

Tracking performance w.r.t. the carriage position z_C for the configurations with underlying pressure or force control have been investigated by experiments at the test-rig of the high-speed linear axis. It is equipped with four pneumatic muscles DMSP-20-1083N from FESTO AG. The internal pressures of the muscles are measured by piezo-resistive pressure sensors, the forces generated by the pneumatic muscles are measured by strain gauges in a full bridge arrangement and the carriage position is determined by a linear incremental encoder with an accuracy of 10 µm. The control algorithm has been implemented on a dSpace real-time system with a sampling time of $T = 1$ ms. The desired trajectories for the carriage position and its corresponding time derivatives are obtained from a trajectory planning module that provides synchronous time optimal trajectories. Here, the desired z-position varies in an interval between -0.3 m and 0.35 m, see upper part of Fig. 4. The maximum velocities are about 1.3 m/s. Thus, nearly the maximal available workspace as well as the maximum achievable velocities are exploited. Fig. 4 also shows the tracking error of the carriage position $e_z = z_{Cd} - z_C$. As can be seen, both control approaches lead to a very good closed-loop performance with maximum control errors during the movements of about 1.5 mm for underlying pressure control and about 2 mm for underlying force control. The steady-state errors are smaller than 0.2 mm for both approaches. To demonstrate the efficiency of the hysteresis compensation strategy as well as the disturbance compensation

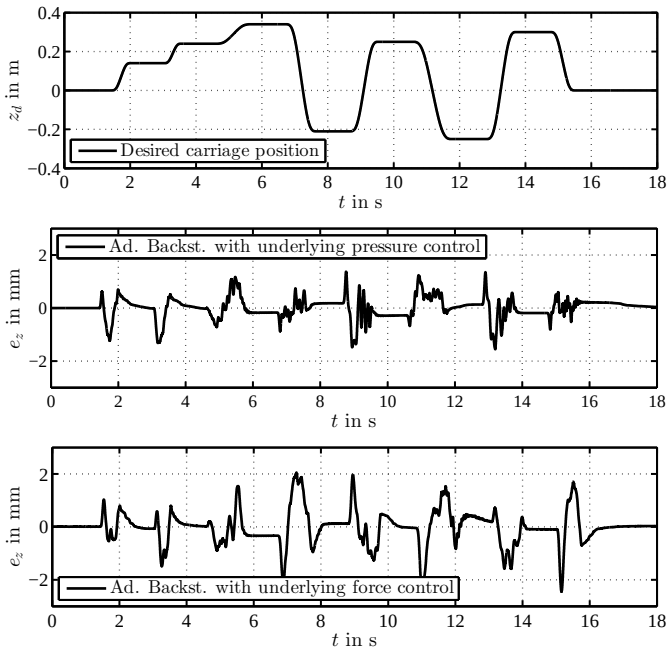

Fig. 4. Desired carriage position (upper part) and corresponding tracking error using adaptive backstepping control with either underlying pressure control (middle part) or underlying force control (lower part).

by adaptive backstepping techniques the tracking error e_z is compared in Fig. 5 and Fig. 6 for the following three cases: a) Backstepping control with disturbance estimation by adaptive backstepping and hysteresis compensation by the ASPI model, b) Backstepping control with hysteresis compensation by the ASPI model – only for the approach with underlying pressure control – and c) pure Backstepping control. As can be seen, the control performance is significantly improved by introducing the hysteresis compensation action based on the ASPI model, and remaining uncertainties are accurately compensated by the adaptive estimation strategy. The corresponding values of the

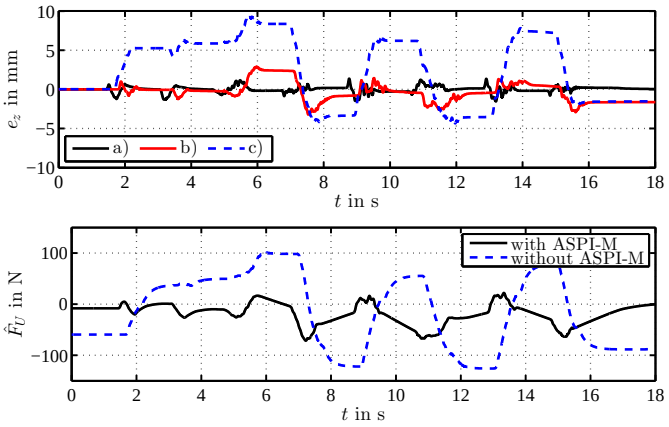

Fig. 5. Upper part: Tracking error for a) Ad. Backstepping with ASPI-M, b) Backstepping with ASPI-M, c) Backstepping. Lower part: Estimated disturbance force. Cascaded control with underlying pressure control.

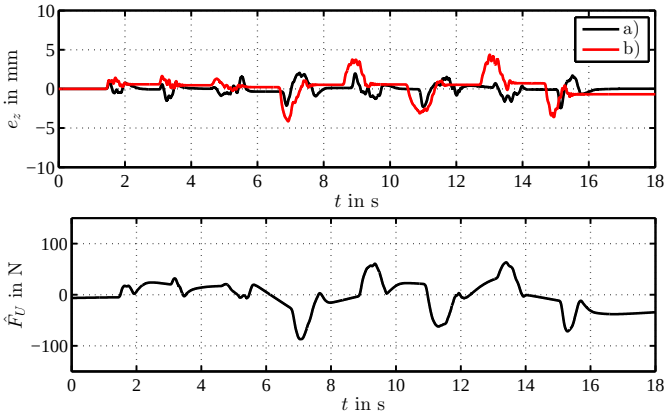

Fig. 6. Upper part: Tracking error for a) Ad. Backstepping, b) Backstepping. Lower part: Estimated disturbance force. Cascaded control with underlying force control.

root mean square error $e_{RMS} = \sqrt{\frac{1}{N}\sum_{i=1}^{N}(z_{Cd}(i) - z_C(i))^2}$ are stated in Table 1. In the lower parts of Fig. 5 and Fig. 6 the estimated disturbance force $\hat{F}_U$ is depicted with and, alternatively, without hysteresis compensation. This demonstrates that a big part of the uncertainties appearing at this test-rig is produced by the hysteresis force of the pneumatic muscles. This explains the superior control behaviour for pure backstepping control in the case of underlying force control compared to the pure backstepping control in the case of underlying pressure control.

	a)	b)	c)
Pressure control	0.37 mm	1.3 mm	4.6 mm
Force control	0.59 mm	–	1.2 mm

Table 1. Root mean square errors for a) Adaptive Backstepping and ASPI-M, b) Backstepping with ASPI-M, c) Backstepping.

7. CONCLUSION

In this paper, two cascaded trajectory control approaches are presented for a new linear axis driven by pneumatic muscles. The first approach involves a fast underlying control of the muscle pressures and an accurate control of the carriage position and the mean muscle force in an outer loop. In the second approach the muscle forces are controlled in a fast underlying control loop, whereas the carriage position and the mean muscle pressure are the controlled variables of the outer loop. For the approach with underlying pressure control the hysteresis in the force characteristic of the pneumatic muscles, which represents the main part of the uncertainties, is compensated by using an asymmetric shifted Prandtl-Ishlinskii model. In contrast, a compensation of the hysteresis is not mandatory in the case of underlying force control; the achieved improvement using hysteresis compensation is only small. Remaining uncertainties are estimated by an adaptive backstepping control. Both control approaches lead to an excellent closed-loop performance with maximum position errors of approximately 2 mm.

REFERENCES

H. Aschemann and D. Schindele. Sliding-mode control of a high-speed linear axis driven by pneumatic muscle actuators. *IEEE Trans. Ind. Electronics*, 55(11):3855–3864, Nov. 2008.

M. Fliess, J. Levine, P. Martin, and P. Rouchon. Flatness and defect of nonlinear systems: Introductory theory and examples. *Int. J. Control*, 61:1327–1361, 1995.

S.V. Krichel, O. Sawodny, and A. Hildebrandt. Tracking control of a pneumatic muscle actuator using one servovalve. *Proc. of ACC 2010, Baltimore, USA*, pages 4385–4390, 2010.

M. Krstić, I. Kanellakopoulos, and P. V. Kokotović. *Nonlinear and Adaptive Control Design*. John Wiley & Sons, 1995.

K. Kuhnen. Modeling, identification and compensation of complex hysteretic nonlinearities: A modified Prandtl-Ishlinskii approach. *European Journal of Control*, 9(4):407–418, 2003.

J. LaSalle and S. Lefschetz. *Stability by Liapunov's Direct Method with Applications*. Academic Press, New York, 1961.

Z. Li, Y. Feng, T. Chai, J. Fu, and Ch.-Y. Su. Modeling and compensation of asymmetric hysteresis nonlinearity for magnetostrictive actuators with an asymmetric shifted Prandtl-Ishlinskii model. *Proceedings of the American Control Conference 2012 (ACC)*, pages 1658–1663, 2012.

J.H. Lilly and L. Yang. Sliding mode control tracking for pneumatic muscle actuators in opposing pair configuration. *IEEE Trans. on Contr. Syst. Techn.*, 13(4):550–558, 2005.

I. D. Mayergoyz. Mathematical models of hysteresis. *IEEE Trans. Magnetics*, 22(5):603–608, 1986.

D. Schindele. *Einsatz pneumatischer Muskeln als Aktoren in der Robotik*. Ph.D. Thesis, University of Rostock (in German), Shaker, Aachen, 2013.

D. Schindele and H. Aschemann. Model-based compensation of hysteresis in the force characteristic of pneumatic muscles. In *Proc. of 12th Int. Workshop on Adv. Mot. Cont., Sarajevo, Bosnia Herzegovina*. 2012.

M. Van-Damme, R. Vanderborght, R. Van Ham, B. Verrelst, F. Daerden, and D. Lefeber. Proxy-based sliding-mode control of a manipulator actuated by pleated pneumatic artificial muscles. *Proc. IEEE Int. Conf. on Robotics and Automation, Rome, Italy*, pages 4355–4360, 2007.

T. Vo-Minh, T. Tjahjowidodo, H. Ramon, and H. Van Brussel. A new approach to modeling hysteresis in a pneumatic artificial muscle using the Maxwell-slip model. *IEEE Transactions on Mechatronics*, 16(1):177–186, 2011.

X. Zhu, G. Tao, B. Yao, and J. Cao. Adaptive robust posture control of a parallel manipulator driven by pneumatic muscles. *Automatica*, 44(9):2248–2257, 2008.